PARAMETRIC ASSESSMENT OF A SOLID OXIDE FUEL CELL-ORGANIC RANKINE CYCLE HYBRID SYSTEM FOR CLEAN POWER GENERATION

by

Ahmed MOUISSI * ***and Rabah TOUAIBI***

Laboratory of Industrial Fluid, Measurements, and Application (FIMA),
University of Khemis, Miliana, Algeria

Original scientific paper
https://doi.org/10.2298/TSCI240603198M

This paper investigates the energy performance of a hybrid system utilizing waste heat from a solid oxide fuel cell to drive an ORC. The study evaluates the ORC performance with various fluids, considering their global warming and ozone depletion potentials. To enhance system efficiency, the ORC is integrated with the solid oxide fuel cell to utilize its waste heat. A comprehensive mathematical model is developed to simulate the coupled system, encompassing all components. This study focuses on the parametric analysis of the ORC, considering crucial working parameters such as operating fluids, evaporator temperature, and pressure ratio. Cogeneration of the solid oxide fuel cell fuel by feeding the ORC increases system performance by 20%. Notably, the R290 fluid emerges as the most efficient among the proposed working fluids. These findings offer valuable insights into hybrid system energy performance, emphasizing the potential for efficiency improvement through waste heat utilization.

Key words: *clean power generation, waste heat recovery, ORC, solid oxide fuel cells, working fluids*

Introduction

In recent decades, researchers and scientists have shown a strong interest in renewable energy as a sustainable solution the world's ever-increasing energy needs. This shift in focus represents a collective effort to redefine our energy consumption patterns in order to reduce the environmental impacts associated with traditional reliance on fossil fuels, particularly the significant CO_2 emissions they generate [1-5]. As such, the main driver of research efforts is the pursuit of discovering and implementing alternative, cleaner sources of energy production that can effectively contribute to reducing climate change and our carbon footprint. The ORC is one of the technologies attracting attention in the search for sustainable energy solutions. This innovative cycle uses the principle of waste heat recovery, making it applicable to a wide range of industries. By recovering heat that would otherwise go unused for examples the geothermal heat [6-8], solar thermal energy [9-12], waste heat from industrial [13], and waste heat from the fuel cells [14-16], the ORC offers not only a path to greater energy efficiency, but also opportunities for cost reduction and environmental stewardship. Its adaptability and scalability make it a promising candidate in the transition a greener, more sustainable energy landscape [17-19]. Although the ORC has established itself

* Corresponding author, e-mail: ahmed.mouissi@univ-dbkm.dz

as a viable technology for recovering low grade waste heat, its relatively modest thermal efficiency is a notable limitation its technical applications. One of the main challenges in improving ORC thermal efficiency is the variance between the temperature-enthalpy profile of the waste heat sources and the organic working fluid used in the ORC system [20, 21]. Addressing this gap is essential to overcoming this obstacle. Additionally, researchers have focused on analyzing the energy efficiencies of ORC modules. Although, researchers have focused on analyzing the energetic efficiencies of ORC modules. Matuszny *et al.* [22] their study focuses on a combined system consisting of a solid oxide fuel cell (SOFC), a hot water storage tank, and an absorption refrigeration cycle. Using modelling software, the thermodynamic properties are evaluated, and a sensitivity analysis is performed. Optimal conditions result in a COP and CCHP efficiency of 0.806 and 85.2% for the LiBr-water system and 0.649 and 83.6% for the NH_3-water system, respectively. In addition, under optimum conditions, the SOFC achieves a net electrical efficiency of 57.5% and a net power output of 123.66 kW. Moreover, Liu *et al.* [16] this study combines an ORC system with a PEMFC cooling water re-circulation system to increase energy efficiency through heat recovery. Comparing R134a and R245fa, R134a is more efficient (11.33% *vs*. 9.16%). Increasing stack temperature improves efficiency, while increasing current density decreases efficiency. Energy efficiency trends are in line with energy efficiency trends. Kumar and Rakshit [17] have introduced a new approach to improve the energy production of a combined SOFC, gas turbine (GT), and ORC system. Their research focused on the use of intercooling heat to increase the energy and exergy efficiency of the system. Their results showed that incorporating an intercooler improved both energy efficiency and exergy performance [23]. In addition, Ragini *et al.* [24] focused on improving energy production processes beyond traditional fossil fuels. Their study focused on a hybrid cycle integrating gas turbines, ORC, and SOFC. Using an ORC with three different working fluids – R141b, R245fa, and R236fa – the system utilizes waste heat from the SOFC-GT system. Simulation results showed an increase in efficiency of between 8% and 12%, with R236fa offering superior performance and efficiency. Touaibi *et al.* [25] this study examines the energy performance of an ORC using three organic fluids: Toluene, R245fa, and R123, and examines how operating temperatures and organic fluid selection affect cycle efficiency. Toluene was found to be the most efficient fluid with an energy efficiency of 7.45%. In addition, the study examines the effect of evaporating temperature on cycle efficiency and shows a significant increase with higher temperatures, most notably for toluene, whose efficiency increases from 10.5% to 21.45% between 80 °C and 150 °C. However, those studies did not consider the environmental impact of the selected working fluids.

Based on the mentioned literature, the aim of this study is to perform a comprehensive parametric and energetic study of an ORC driven by waste heat generated by a SOFC. In particular, the study introduces a novel approach by carefully selecting working fluids according to their ozone depletion potential (ODP) and global warming potential (GWP). The selected fluids include R290, R152a, R600, and R245Fa. In addition, research is focused on optimizing overall system efficiency by integrating the SOFC and efficiently recovering its waste heat. This multi-faceted approach is expected to provide valuable information on how to improve energy conversion efficiency while considering environmental sustainability factors.

Numerical model

The SOFC is a versatile technology that can be powered by a variety of fuels, making it a promising option for clean energy production. In this study the operation parameters of the SOFC remain constant.

Figure 1 shows the basic diagram of a system combining an SOFC fuel cell and an ORC. Each component is shown to reflect the arrangement of SOFC, turbine, condenser, pump, heat recovery boilers, compressors, and heat exchangers. Ambient air is compressed from Point 1 to Point 2, then passes through a heat exchanger to be heated at Point 3 before entering the solid plate fuel cell cathode. Methane gas is also compressed from Point 4 to Point 5, then passed through a heat exchanger and heated at Point 6. Similarly, water is pumped from Point 8 to Point 9, heated at Point 10 using the same technology, and then mixed with fuel at Point 7 to produce hydrogen gas, which feeds the anode. After mixing with the fuel circulating from Point 6 to Point 7, the mixture reacts to produce hydrogen gas, which is used to power the anode. The gas emitted by the anode and cathode, at Points 11 and 12, respectively, is then sent to a thermal transformer to recover heat from the evaporator, which is used to supply a power circuit to operate this cycle. The operating parameters of the SOFC and the ORC are showed in tab. 1 [26].

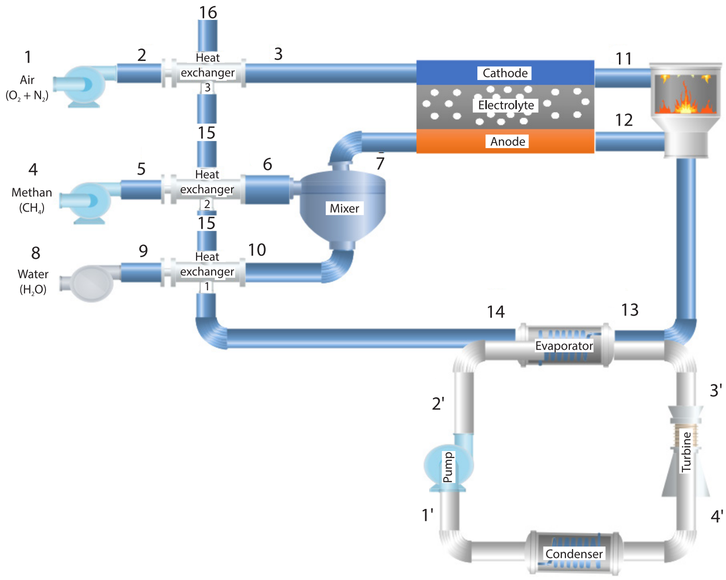

Figure 1. Schematic design for the suggested system

The thermophysical properties of the suggested organic fluids used as working fluids in the ORC are listed in tab. 2 [27].

Several assumptions were made to model the system [28, 29]:

- The composition of the air is assumed to be 21% O and 79% N.
- All substances are treated as ideal gases.
- The system operates in a steady-state.
- The SOFC is assumed to be adiabatic with respect to the environment.
- The methane reforming reaction is assumed to be complete, so there is no methane at the mixer outlet.
- The SOFC inlet and outlet are assumed to have the same temperature and pressure.
- The temperature difference between the inlet and outlet is kept constant.
- Turbines, compressors, and pumps are assumed to be adiabatic with isentropic efficiencies.
- The evaporator and condenser outlet flows are assumed to be saturated.

Table 1. System operating conditions

Parameter	Value	Unit
R_{cont}	0	[Ωm²]
L_{an}	$5 \cdot 10^{-4}$	[m]
L_{ca}	$5 \cdot 10^{-5}$	[m]
L_e	$1 \cdot 10^{-5}$	[m]
L_{int}	$3 \cdot 10^{-3}$	[m]
A_{cell}	0.01	[m²]
N_{FC}	11000	[–]
R_{stc}	2.5	[–]
F	96485	[–]
U_f	0.75	[–]
U_a	0.15	[–]
j	8000	[Am^{-2}]
T_{Pc}	873	[K]
P_{ref}	101.15	[KPa·s]
Pressure drops in the stack	2	[%]
Pressure drops in the exchanger	3	[%]
τ_{Ca}	1.19	[–]
τ_{Cc}	1.19	[–]
LHV_{CH4}	802361	[Jmol^{-1}]
ORC		
Evaporator temperature	90	[°C]
Isentropic pump efficiency	0.9	[–]
Isentropic turbine efficiency	0.85	[–]
Low pressure	100	[kPa]
High pressure	1000	[kPa]

Table 2. Thermophysical properties of the four organic fluids

Working fluids	R1270	R-600	R-290	R-245Fa
Chemical formula	C_3H_6	C_4H_{10}	C_3H_8	$C_3H_3F_5$
Molar mass [kgmol^{-1}]	42.08	58.1	44.10	134.05
Critical temperature [°C]	92	152	370	154
Critical pressure [bar]	46.6	36.709	42.5	36.5
ODP	0	0	0	0
GWP	0	3	<10	950

System modelling

To simulate the SOFC performance, an electrochemical model incorporating the Butler-Volmer equation, Fick's model, and Ohm's law was employed. This model accounted for activation, concentration, and ohmic losses, respectively. The generated energy of the SOFC is written:

$$P_{\text{out}} = N_{\text{cell}} \times V_{\text{SOFC}} \times j \times A_{\text{cell}} \tag{1}$$

where N_{cell} is the number of cells, A_{cell} – the area of cell, and V_{SOFC} – the overall voltage.

The considered voltages are shown in tab. 3 [30-32]:

$$V_{\text{SOFC}} = E_{\text{nernst}} - V_{\text{act}} - V_{\text{conc}} - V_{\text{ohmic}} \tag{2}$$

Table 3. Voltage calculation

Voltage	Equation
Nernst reversible voltage	$E_{\text{nernst}}=E_0+\dfrac{\text{R}T}{2\text{F}}\ln\left(\dfrac{P_{\text{H}_2}P_{\text{O}_2}^{0.5}}{P_{\text{H}_2\text{O}}}\right)$
Activation losses	$V_{\text{act}} = V_{\text{act,an}} + V_{\text{act,ca}}$
	$V_{\text{act,an}} = \dfrac{\text{R}T}{2\text{F}}\sinh^{-1}\left(\dfrac{j}{2\cdot 0.65\cdot 10^4}\right)$
	$V_{\text{act,ca}} = \dfrac{\text{R}T}{2\text{F}}\sinh^{-1}\left(\dfrac{j}{2\cdot 0.25\cdot 10^4}\right)$
Ohmic losses	$V_{\text{ohm}} = \left(R_{\text{contact}} + \rho_{\text{an}}L_{\text{an}} + \rho_{\text{ca}}L_{\text{ca}} + \rho_{\text{e}}L_{\text{e}} + \rho_{\text{int}}L_{\text{int}}\right)j$
Concentration losses	$V_{\text{act}} = V_{\text{conc,an}} + V_{\text{conc,ca}}$
	$V_{\text{conc,an}} = -\dfrac{\text{R}T}{2\text{F}}\left[\ln\left(1-\dfrac{j}{j_{\text{as}}}\right)+\ln\left(1+\dfrac{P_{\text{H}_2}j}{P_{\text{H}_2\text{O}}j_{\text{an}}}\right)\right]$
	$V_{\text{conc,ca}} = -\dfrac{\text{R}T}{2\text{F}}\ln\left(1-\dfrac{j}{j_{\text{ca}}}\right)$

Thermodynamic model

Thermodynamic modelling is performed, and mass balances are defined [33]:

$$\sum \dot{m}_{\text{in}} = \sum \dot{m}_{\text{out}} \tag{3}$$

The First law of thermodynamics is used to formulate the energy balance of any system and is written in general terms:

$$\sum \dot{m}_{\text{in}} h_{\text{in}} + \sum \dot{Q}_{\text{in}} + \sum \dot{W}_{\text{in}} = \sum \dot{m}_{\text{out}} h_{\text{out}} + \sum \dot{Q}_{\text{out}} + \sum \dot{W}_{\text{out}} \tag{4}$$

Using the ORC-SOFC system and the principles of the First law of thermodynamics as a foundation, tab. 4 shows the system performance parameters.

Table 4. System performance parameters

Term	Equation
SOFC AC power	$\dot{W}_{SOFC,AC} = P_{out}\eta_{inv}$
Air compressor	$\dot{W}_{AC} = \dot{m}(h_2 - h_1)$
Fuel compressor	$\dot{W}_{FC} = \dot{m}(h_5 - h_4)$
Water pump	$\dot{W}_{wp} = \dot{m}(h_9 - h_8)$
Net electrical power	$\dot{W}_{SOFC,net} = \dot{W}_{SOFC,AC} - \left(\dot{W}_{AC} + \dot{W}_{FC} + \dot{W}_{wp}\right)$
The SOFC energy efficiency	$\eta_{FC} = \dfrac{\dot{W}_{SOFC}}{\dot{m}_{CH_4} LHV_{CH_4}} \times 100$
ORC power	$\dot{W}_{ORC} = \dot{m}\left(h_4 - h_3\right)$
ORC Net power	$\dot{W}_{ORC,net} = W_{ORC} - W_{FP}$
HRSG input energy	$\dot{Q}_{in,HRSG} = \dot{m}_{14}h_{14} - \dot{m}_{3'}h_{3'}$
The ORC energy efficiency	$\eta_{ORC} = \dfrac{W_{ORC,net}}{\dot{Q}_{in,HRSG}}$
System efficiency	$\eta_{FC} = \dfrac{\dot{W}_{SOFC} + \dot{W}_{ORC,net}}{\dot{m}_{CH_4} LHV_{CH_4}}$

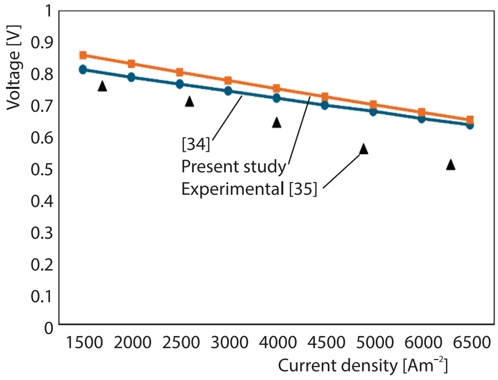

Figure 2. Validation of the proposed SOFC model

Validation

To validate the simulated SOFC configuration, a comparative analysis was performed with the theoretical study of Bafekr *et al.* [34] and the experimental investigation of Tao *et al.* [35]. A comprehensive review of the relevant literature was conducted to validate the SOFC model [34, 35]. The polarization validation is shown graphically in fig. 2, which illustrates the variation of voltage *vs.* current density.

Results and discussion

Effect of evaporator temperature

This section examines the effect of evaporator temperature on ORC and overall system performance. In addition, all proposed working fluids for the ORC are examined to assess their effect on system performance. Figure 3 illustrates the effect of evaporator temperature on ORC system performance with four organic fluids. For each organic fluid, the effect of evaporator temperature was studied by varying it from 50-110 °C. The results show that increasing the evaporator temperature significantly increases the power produced by the organic Rankine cycle. According to the data, the R290 fluid stands out as the most efficient, generating an optimum power of 150 W at 50 °C, which increases proportionally to reach its maximum value of 190 W at 90 °C. Next, the R152a fluid performed in the same evaporation temperature range, with an initial power of 130 W that increases proportionally to about 180 W. Results for the R600 fluid follow, with power ranging from 85 W to 110 W in the same evaporation temperature range, while those for the R245Fa fluid, with lower power, are between 65 W and 90 W. moreover the fig. 3 shows the evolution of the power produced by the combined ORC-SOFC system as a function of the evaporator temperature. The results show a simultaneous increase in power as the evaporator temperature increases. The R290 fluid in the ORC stands out as the best performer, with an initial power of 720 kW at 50 °C, gradually increasing to 750 kW at 90 °C. Similarly, the use of R152a fluid in the same temperature range gives very good results, with an initial power of 700 kW and a proportional increase to about 740 kW. Next, the results for the R600 fluid show a power range from 660-720 kW in the same temperature range, followed by the R245Fa fluid which gives a lower power in the same temperature range, from 630-699 kW.

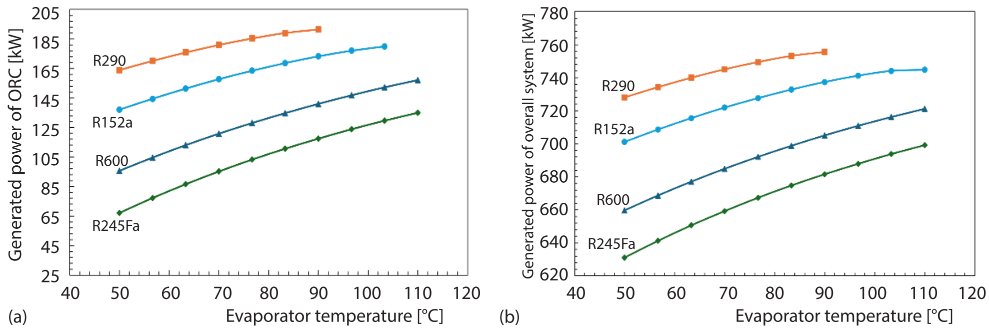

Figure 3. Effect of the evaporator temperature on the ORC power output and the overall system

Figure 4 illustrates the effect of evaporator temperature on the efficiency of the ORC cycle. The efficiency of the ORC increases proportionally with increasing evaporator temperature, ranging from 0.23-0.26 as the temperature increases from 50-90 °C when R290 fluid is used in the cycle. When R152a is used, the cycle efficiency increases proportionally with increasing temperature from 0.19-0.25. When R600 fluid is used, the cycle efficiency varies between 0.13 and 0.22 over the same temperature range, while with R245Fa the efficiency varies between 0.09 and 0.19. In addition fig. 4 shows the evaporator temperature affects the efficiency of the combined system. In fact, an increase in evaporator temperature results in an improvement in system efficiency. For the organic fluid R290, the system efficiency increases

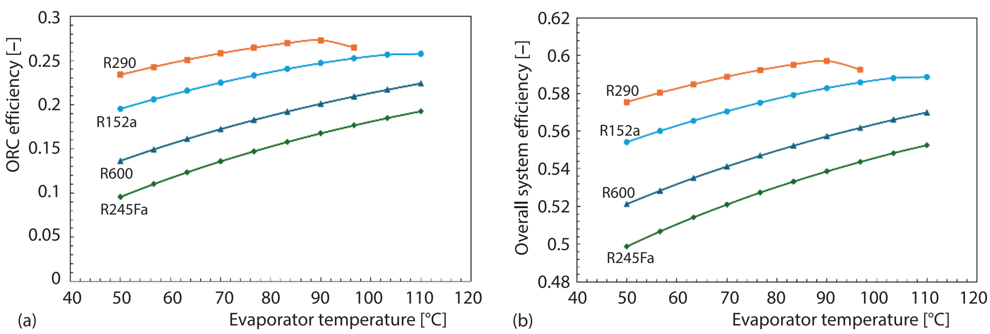

Figure 4. Effect of evaporator temperature on ORC and overall system efficiency

from 0.57-0.59 as the evaporator temperature increases from 50-90 °C. For R152a, the cycle efficiency increases proportionally with temperature, from 0.55-0.58. Results for R600 show efficiencies ranging from 0.52-0.56 over the same temperature range, while for R245Fa efficiencies range from 0.49-0.55 over the same temperature range.

Effect of compression ratio

According to fig. 5, the effect of increasing the compression ratio on the power produced by the ORC varies according to the organic fluids used. The R290 fluid produces the highest power, ranging from 188-192 kW, while the results obtained with the R152a fluid are satisfactory, with a power ranging from 170-174 kW. The results obtained with R600 fluid are around 141 kW, followed by those obtained with R245Fa fluid, which reach around 118 kW. In all cases, a slight reduction in the power generated by the cycle is observed as the compression ratio increases. As shown in fig. 5, the effect of increasing the compression ratio on the power output of the combined SOFC/ORC system varies with the organic fluids used in the Rankine cycle. The R290 fluid achieves the highest power output, ranging from 752-756 kW. The results obtained with R152a are satisfactory, ranging from 734-730 kW. The results obtained with R600 fluid are around 706 kW, followed by those obtained with R245Fa fluid, which reach around 683 kW.

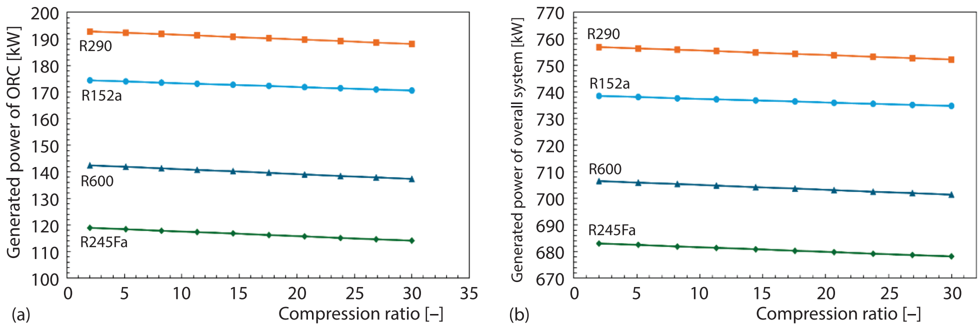

Figure 5. Effect of compression ratio on the generated power of the ORC and overall system

Figure 6 shows the effect of increasing the compression ratio on the efficiency of the ORC cycle using different organic fluids in the cycle. The cycle efficiency peaks when R290 fluid is used in the Rankine cycle at 0.27. This is followed by R152a at 0.24, R600 at 0.2, and R245Fa at 0.15. Moreover fig. 6 illustrates the effect of increasing the compression ratio on the efficiency of the combined SOFC/ORC system using different organic fluids in the organic

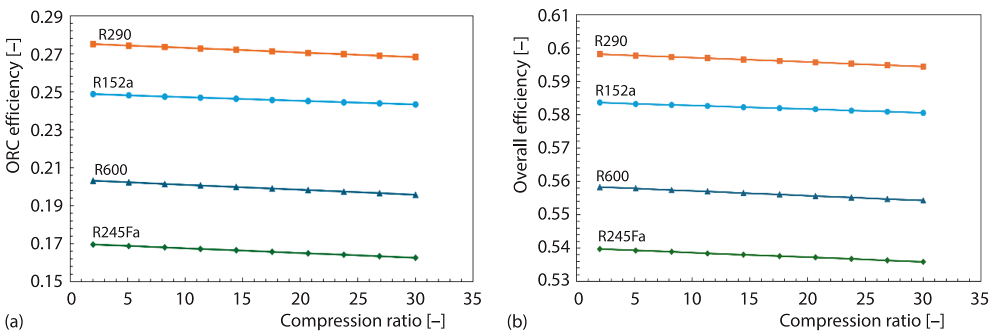

Figure 6. Effect of compression ratio on the ORC and overall system efficiency

Rankine cycle. It can be seen that the use of R290 fluid in the Rankine cycle leads to a maximum efficiency of 0.59, followed by the use of R152a fluid with an efficiency of 0.58, then the use of R600 fluid with an efficiency of 0.55, and finally the use of R245fa fluid with an efficiency of 0.53.

Conclusions

This study examines the results of a cogeneration system integrating an SOFC and an ORC. Several parameters were evaluated, including evaporator temperature and ORC compression ratio, as well as several environmental fluids. The results of the study are as follows.

- The results show that increasing the evaporator temperature increases the performance of the ORC, with variations depending on the organic fluids used. The R290 fluid stands out as having the best performance, followed by the R152a, R600, and R245Fa fluids.
- The study also showed that evaporator temperature affects the efficiency of the combined system, with an increase in evaporator temperature leading to an improvement in overall system efficiency. It is also noteworthy that all four organic fluids show a slight decrease in cycle power and overall efficiency as the compression ratio increases.
- These results highlight the importance of organic fluid selection and compression ratio in the design and optimization of integrated ORC systems with SOFC. Finally, these results have significant implications for energy applications, providing valuable information on the potential performance of different organic fluids in integrated ORC/SOFC systems, as well as the benefits of compression ratio optimization.

Nomenclature

A_{cell} – activation cell area, [m^2]
$E_{nenrnst}$ – Nernst reversible voltage, [V]
j – current density, [Am^{-2}]
F – Faraday number, [Cmol^{-1}]
L – thickness of SOFC layer, [m]
LHV – lower heating value, [Jmol^{-1}]
$\dot{m}$ – mole rate, [mols^{-1}]
N_{cell} – number of the fuel cell stack, [–]
P_i – partial pressure, [bar]
P_{out} – generated power of the fuel cell, [kW]
$\dot{Q}$ – heat rate, [kW]
R – ideal gas constant, [Jmol^{-1}K^{-1}]
T – temperature, [K]
V – voltage, [V]
W – work rate, [kW]

Greek symbols

η – efficiency, [%]
ρ – ohmic resistance, [ohm]

Subscripts

an – anode
ca – cathode

References

[1] Cui, D., *et al*., China's Non-Fossil Fuel CO_2 Emissions from Industrial Processes, *Applied Energy*, *254* (2019), 113537
[2] Peters, G. P., *et al*., Carbon Dioxide Emissions Continue to Grow Amidst Slowly Emerging Climate Policies, *Nature Climate Change*, *10* (2020), Dec., pp. 3-6
[3] Martins, F., *et al*., Analysis of Fossil Fuel Energy Consumption and Environmental Impacts in European Countries, *Energies*, *12* (2019), 6, 964
[4] Sugiawan, Y., Managi, S., New Evidence of Energy-Growth Nexus from Inclusive Wealth, Renewable and Sustainable Energy Reviews, *103* (2019), Apr., pp. 40-48
[5] Tan, Q., *et al*., Risks, Challenges and Strategies of Power Systems Against the Background of Carbon Neutrality, *Clean Energy*, *7* (2023), 4, pp. 767-782
[6] Maali, R., Khir, T., Performance Analysis of Different ORC Power Plant Configurations Using Solar and Geothermal Heat Sources, *International Journal of Green Energy*, *17* (2020), 6, pp. 349-362
[7] Loni, R., *et al*., A Critical Review of Power Generation Using Geothermal-Driven Organic Rankine Cycle, *Thermal Science and Engineering Progress*, *25* (2021), 101028

[8] Atia, D. M., *et al*., Organic Rankine Cycle Based Geothermal Energy for Power Generation in Egypt, *Energy and Power Engineering*, *09* (2017), 12, pp. 814-828
[9] Mahmood, H., Hossin, K., Daily, Monthly and Annual Thermal Performance of a Linear Fresnel Reflector to Drive An Organic Rankine-Cycle System, *Clean Energy*, *5* (2021), 4, pp. 673-689
[10] Mahlia, T. M. I., *et al*., Organic Rankine Cycle (ORC) System Applications for Solar Energy: Recent Technological Advances, *Energies*, *12* (2019), 15
[11] Wang, R., *et al*., Comparative Analysis of Small-Scale Organic Rankine Cycle Systems for Solar Energy Utilisation, *Energies*, *12* (2019), 5
[12] Almohammadi, B. A., *et al*., Energy Analysis of a Novel Solar Tri-Generation System Using Different ORC Working Fluids, *Case Studies in Thermal Engineering*, *45* (2023), 102918
[13] Loni, R., *et al.*, A Review of Industrial Waste Heat Recovery System for Power Generation with Organic Rankine Cycle: Recent Challenges and Future Outlook, *Journal of Cleaner Production*, *287* (2021), 125070
[14] Al-Sulaiman, F. A., *et al*., Performance Comparison of Three Trigeneration Systems Using Organic Rankine Cycles, *Energy*, *36* (2011), 9, pp. 5741-5754
[15] Ebrahimi, M., Moradpoor, I., Combined Solid Oxide Fuel Cell, Micro-Gas Turbine and Organic Rankine Cycle for Power Generation (SOFC-MGT-ORC), *Energy Conversion and Management*, *116* (2016), May, pp. 120-133
[16] Liu, C., *et a*l., Analysis of a Combined Proton Exchange Membrane Fuel Cell and Organic Rankine Cycle System for Waste Heat Recovery, *International Journal of Green Energy*, *18* (2020), 3, pp. 271-281
[17] Kumar, A., Rakshit, D., A Critical Review on Waste Heat Recovery Utilization with Special Focus on Organic Rankine Cycle Applications, *Cleaner Engineering and Technology*, 5 (2021), 100292
[18] Mahmoudi, A., *et al.*, A Recent Review of Waste Heat Recovery by Organic Rankine Cycle, *Applied Thermal Engineering*, *143* (2018), Oct., pp. 660-675
[19] Zhao, Y., *et al*., Expansion Devices for Organic Rankine Cycle (ORC) Using in Low Temperature Heat Recovery: A Review, *Energy Conversion and Management*, *199* (2019), 111944
[20] Emadi, M. A., *et al*., Working-Fluid Selection And Thermoeconomic Optimisation Of A Combined Cycle Cogeneration Dual-Loop Organic Rankine Cycle (ORC) System for Solid Oxide Fuel Cell (SOFC) Waste-Heat Recovery, *Applied Energy*, *261* (2020), 114384
[21] Matthew, O., Nieh, S., Effects of ORC Working Fluids on Combined Cycle Integrated with SOFC and ORC for Stationary Power Generation, *Energy and Power Engineering*, *11* (2019), 04, pp. 167-185
[22] Matuszny, K., *et al.*, Integration of Solid-Oxide Fuel Cells And Absorption Refrigeration for Efficient Combined Cooling, Heat and Power Production, *Clean Energy*, *4* (2020), 4, pp. 328-348
[23] Kumar, P., *et al*., Thermodynamic Assessment of a Novel SOFC and Intercooled GT Integration with ORC: Energy and Exergy Analysis, *Thermal Science and Engineering Progres*s, *34* (2022), 101411
[24] Singh, R., Singh, O., Comparative Study of Combined Solid Oxide Fuel Cell-Gas Turbine-Organic Rankine Cycle for Different Working Fluid in Bottoming Cycle, *Energy Conversion and Management*, *171* (2018), Sept., pp. 659-670
[25] Touaibi, R., *et al*., An Energy Investigation of an Organic Rankine Cycle Utilizing Three Organic Fluids, *Hittite Journal of Science and Engineering*, *7* (2020), 1, pp. 41-44
[26] Adebayo, V., *et al*., Energy, Exergy and Exergo-Environmental Impact Assessment of a Solid Oxide Fuel Cell Coupled with Absorption Chiller and Cascaded Closed Loop ORC for Multi-Generation, *International Journal of Hydrogen Energy*, *47* (2022), 5, pp. 3248-3265
[27] Bahrami, M., *et al.*, Low Global Warming Potential (GWP) working Fluids (WFs) for Organic Rankine Cycle (ORC) Applications, *Energy Reports*, *8* (2022), Nov., pp. 2976-2988
[28] Colpan, C., *et al*., Thermodynamic Modelling of Direct Internal Reforming Solid Oxide Fuel Cells Operating with Syngas, *International Journal of Hydrogen Energy*, *32* (2007), 7, pp. 787-795
[29] Adebayo, V., *et al*., Energy, Exergy and Exergo-Environmental Impact Assessment of a Solid Oxide Fuel Cell Coupled with Absorption Chiller and Cascaded Closed Loop ORC for Multi-Generation, *International Journal of Hydrogen Energy*, *47* (2022), 5, pp. 3248-3265
[30] Erdogan, A., *et al*., Analysis of Reformate Syngas Mixture Fed Solid Oxide Fuel Cell through Experimental and 0-D Thermodynamic Modelling Studies, *International Journal of Hydrogen Energy*, *48* (2023), 60, pp. 23110-23126
[31] Lee, T. S., *et al*., Design and Optimization of a Combined Fuel Reforming and Solid Oxide Fuel Cell System with Anode off-Gas Recycling, *Energy Conversion and Managemen*t, *52* (2011), 10, pp. 3214-3226
[32] Ranjbar, F., *et al*., Energy and Exergy Assessments of a Novel Trigeneration System Based on a Solid Oxide Fuel Cell, *Energy Conversion and Management*, *87* (2014), Nov., pp. 318-327

[33] Grasham, O., *et al*., Combined Ammonia Recovery and Solid Oxide Fuel Cell Use at Wastewater Treatment Plants for Energy and Greenhouse Gas Emission Improvements, *Applied Energy*, *240* (2019), Apr., pp. 698-708

[34] Bafekr, S. H., *et al.*, Thermo-Electrochemical Modelling of Oxygen Ion-Conducting Solid Oxide Fuel Cells with Internal Steam Reforming in the Water-Energy Nexus, *Energy Nexus*, *5* (2022), 100057

[35] Tao, G., *et al*., Intermediate Temperature Solid Oxide Fuel Cell (IT-SOFC) Research and Development Activities at MSRI, *Proceedongs*, in 19th Annual ACERC and ICES Conference, Provo, Ut., USA, 2005

Paper submitted: June 3, 2024
Paper revised: Juky 24, 2024
Paper accepted: August 1, 2024